CHAPTER

4

Electrical Excitability and Ion Channels

Bertil Hille, William A. Catterall

OUTLINE

The nervous system enables animals to receive and act on internal and external stimuli with speed and coordination. Activities of the nervous system are reflected in ongoing electrical and chemical signals. Consider a simple reflex arc mediating reflex withdrawal of the leg from a painful stimulus. Several cell types are involved in a network, shown diagrammatically in Figure 4-1. Messages travel from skin receptors through the network as a volley of electrical disturbances, terminating in contraction of specific muscles. This chapter concerns the origin of electrical potentials in such excitable cells—potentials generated by the passive diffusion of Na^+, K^+, Ca^{2+} and Cl^- ions through highly selective molecular pores in the cell plasma membrane called ion channels. Such channels play a role in membrane excitation that is as central as the role of enzymes in metabolism. The opening and closing of specific ion channels shape the membrane potential changes. The interested reader is referred to Hodgkin and Huxley (1964), Armstrong (2003), Nicholls et al. (2001) and Hille (1997, 2001) for more detailed treatment of this subject. Over 500 human genes coding for subunits of ion channels have been identified.

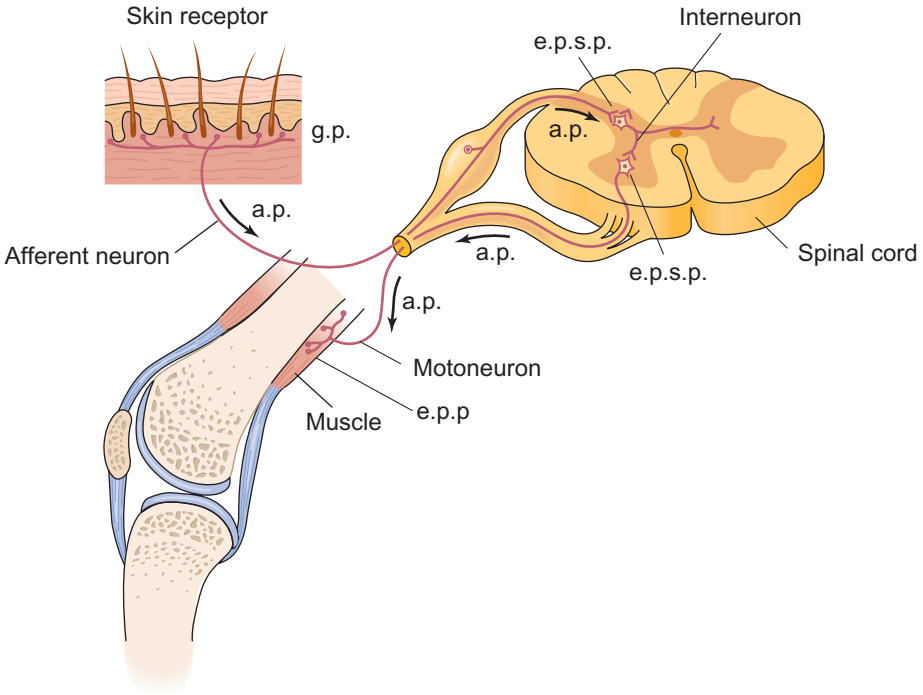

FIGURE 4-1 **Path of excitation in a simplified spinal reflex that mediates withdrawal of the leg from a painful stimulus.** In each of the three neurons and in the muscle cell, excitation starts with a localized slow potential and is propagated via an action potential (*a.p.*). Slow potentials are the generator potential (*g.p.*) at the skin receptor; the excitatory postsynaptic potentials (*e.p.s.p.*) in the interneuron and motoneuron, and the end-plate potential (*e.p.p.*) at the neuromuscular junction. Each neuron makes additional connections to other pathways that are not shown.

MEMBRANE POTENTIALS AND ELECTRICAL SIGNALS IN EXCITABLE CELLS

Excitable cells have a negative membrane potential

Before examining the variety of electrical signals, consider the electrochemical theory behind their generation. At rest, the cytoplasm is electrically more negative than the external bathing fluid by 30–100 mV. This potential drop occurs across the cell's plasma membrane, as is revealed by recording with an electrolyte-filled glass pipette microelectrode. When the sharp tip of such an electrode passes through the plasma membrane, it reports a sudden negative drop, the resting potential of the cell. By convention, the membrane potential is defined as 'inside' minus 'outside,' so the resting potential is a negative number. Signals that make the cytoplasm more positive than it is at rest are said to depolarize the membrane, and those making it more negative are said to hyperpolarize the membrane.

Membrane potentials arise from the diffusion of ions (Nicholls et al., 2001; Hille, 1997; 2001). Consider the electrolyte system represented in Figure 4-2 (left), where a porous membrane separates aqueous solutions of unequal concentrations of a fictitious salt KA. Assume that the membrane pores are permeable exclusively to K^+ so that K^+ begins to diffuse across the membrane but A^- does not. Initially the movement of K^+ from the concentrated side to the dilute side exceeds the movement in the reverse direction, so a few K^+ ions flow down

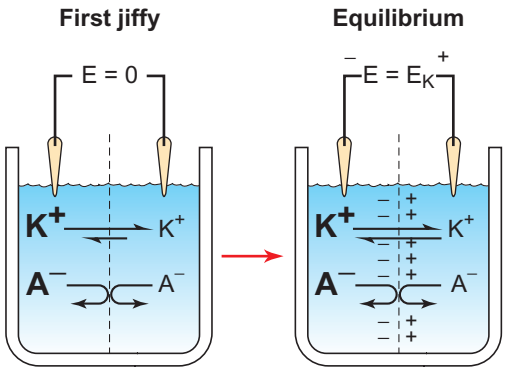

FIGURE 4-2 **Origin of the membrane potential in a purely K^+-permeable membrane.** The porous membrane separates unequal concentrations of the dissociated salt K^+A^-. In the first 'jiffy,' the membrane potential, E, recorded by the electrodes above is zero and K^+ diffuses to the right down the concentration gradient. The anion A^- cannot cross the membrane, so a net positive charge builds up on the right and a negative charge on the left. At equilibrium, the membrane potential, caused by the charge separation, has built up to the Nernst potential, E_K, where the fluxes of K^+ become equal in the two directions.

their concentration gradient. This process does not continue for long, because each K^+ ion carries a positive charge from one compartment to the other and leaves a net negative charge behind. The growing separation of charge creates an electrical potential difference (the membrane potential) between the two solutions. The accumulated positive charge on the side

into which the K^+ ions diffuse sets up an electrical force that opposes further net movement of K^+, and soon the membrane potential stops changing. The membrane potential reached in a system with only one permeant ion and no perturbing forces is called the equilibrium, or Nernst, potential for that ion; thus, the final membrane potential for the system in Figure 4-2 is the K^+ equilibrium potential E_K. At that potential, there is no further net movement of K^+, and unless otherwise disturbed, the membrane potential and ion gradient will remain stable indefinitely. The value of the Nernst potential is derived from thermodynamics by recognizing that the change of electrochemical potential $\Delta\mu_j$, for moving the permeant ion j^{+z} across the membrane, must be zero at equilibrium:

$$\Delta\mu_j = 0 = RT \ln \frac{[j]_o}{[j]_i} - zFE \qquad (1)$$

where R is the gas constant (8.31 J)/°/mol, T is absolute temperature in Kelvin (°C + 273.2), and F is Faraday's constant (96,500 C/mol). Using terms appropriate to biology, $[j]_o$ and $[j]_i$ represent activities of ion j^{+z} outside and inside a cell; z is the ionic valence; and E the membrane potential, defined as 'inside minus outside'. Solving for E, and calling it E_j to denote the ion at equilibrium gives the Nernst equation for j:

$$E_j = \frac{RT}{zF} \ln \frac{[j]_o}{[j]_i}. \qquad (2)$$

For practical use at 20°C, the Nernst equation can be rewritten

$$E_j = \frac{58\,\text{mV}}{z} \log_{10} \frac{[j]_o}{[j]_i}, \qquad (3)$$

showing that for a 10:1 transmembrane gradient, a monovalent ion can give rise to 58 mV of membrane potential. Table 4-1 gives approximate intracellular and extracellular concentrations of the four electrically most important ions in a mammalian skeletal muscle cell and the Nernst potentials calculated from these numbers at 37°C (neglecting possible activity coefficient corrections). Experimentally it is found that the resting muscle membrane is primarily permeable to K^+ and Cl^- and, therefore, the resting potential in muscle is −90 mV, close to the equilibrium potentials E_K and E_{Cl}. To summarize, membrane potentials arise by diffusion of a small number of ions down their concentration gradient across a permselective membrane.

Real cells are not at equilibrium

Although the concept of equilibrium potentials is essential to understanding and predicting the membrane potentials generated by ion permeability, real cells actually never are at equilibrium, because different ion channels open and close during excitation, and even at rest several types of channels are open simultaneously. Under these circumstances, the ion gradients are dissipated constantly, albeit slowly, and ion pumps are always needed in the long run to maintain a steady state (see Ch. 3). When the membrane is permeable to several ions, the steady-state potential is given by the sum of contributions of the permeant ions, weighted according to their relative permeabilities P_j:

$$E = \frac{RT}{F} \ln \frac{P_{Na}[Na^+]_o + P_K[K^+]_o + P_{Cl}[Cl^-]_i}{P_{Na}[Na^+]_i + P_K[K^+]_i + P_{Cl}[Cl^-]_o}. \qquad (4)$$

This Goldman–Hodgkin–Katz voltage equation is often used to determine the relative permeabilities of ions from experiments where the bathing ion concentrations are varied and changes in the membrane potential are recorded (Hille, 2001).

TABLE 4-1 Approximate Free Ion Concentrations in Mammalian Skeletal Muscle

Ion	Extracellular concentration (mmol/l)	Intracellular concentration (mmol/l)	$[Ion]_o/[Ion]_i$	Nernst potential* (mV)
Na^+	145	12	12	+66
K^+	4	155	0.026	−97
Ca^{2+}	1.5	$<10^{-3}$	>1,500	>97
Cl^-	120	4†	30†	−90†

*Equilibrium potentials calculated at 37°C from the Nernst equation.
†Calculated assuming a −90 mV resting potential for the muscle membrane and assuming that chloride ions are at equilibrium at rest.

Transport systems may also produce membrane potentials

The equations just discussed describe passive electrodiffusion in ion channels where the only motive forces on ions are thermal and electrical, and they explain almost all the potentials of excitable cells. However, one other class of electric current source in cells can generate potentials: the ion pumps and other membrane transporters that couple ion movements to the movements of other molecules. In excitable cells, the most prominent is the Na^+/K^+ pump (see Ch. 3), which gives a net export of positive charge and hence can hyperpolarize the plasma membrane slightly in proportion to the rate of pumping (Nicholls et al., 2001); but hyperpolarization from this electrogenic pumping is at most a few millivolts. By contrast, mitochondria (and plant, algal, fungal, and bacterial cells) have powerful current sources in their proton transport system. Their membrane potentials are often dominated by this electrogenic system and cannot be described in terms of diffusion in passive ion channels.

Electrical signals recorded from cells are of two types: stereotyped action potentials and a variety of slow potentials

The action potential of axons is a brief, spike-like depolarization that propagates regeneratively as an electrical wave

without decrement and at a high, constant velocity from one end of the axon to the other (Hodgkin, 1964; Nicholls et al., 2001). It is used for all rapid signaling over a distance. For example, in the reflex arc of Figure 4-1 action potentials in motor axons would carry the message from spinal cord to leg, telling some muscle fibers of the biceps femoris to contract. In large mammalian axons at body temperature, the action potential at any one patch of membrane may last only 0.4 ms as it propagates at a speed of 100 m/s. The action potential is normally elicited when the cell membrane is depolarized beyond a threshold level; and it is said to arise in an all-or-nothing manner because a subthreshold stimulus gives no propagated response, whereas every suprathreshold stimulus elicits the stereotyped propagating wave. Underlying the propagated action potential is a regenerative wave of opening and closing of voltage-gated ion channels that sweeps along the axon. Action potentials are also frequently referred to as spikes or impulses. Most nerve and muscle cells and many endocrine cells can make action potentials.

By contrast, slow potentials are localized membrane depolarizations and hyperpolarizations, with time courses ranging from several milliseconds to minutes. They are associated with a variety of transduction mechanisms. For example, slow potentials arise postsynaptically at the sites of action of neurotransmitter molecules (see Ch. 12) and in transduction sites of sensory receptors (see Chs. 51–54). Slow potentials are graded in relation to their stimulus and sum with each other within the cell while decaying passively over a distance of no more than a few millimeters from their site of generation. Underlying the slow potential is a graded and local opening or closing of ion channels reflecting the intensity of the stimulus. These channels are gated by stimuli other than voltage. The natural stimulus for the initiation of propagated action potentials is a depolarizing slow potential exceeding the firing threshold. In each of the cell types involved in the reflex arc in Figure 4-1, depolarizing slow potentials initiate propagating action potentials as the message moves forward.

ACTION POTENTIALS IN ELECTRICALLY EXCITABLE CELLS

During excitation, ion channels open and close and a few ions flow

The membrane potential does not change unless there is a net charge movement across the membrane. During a propagated action potential, ion channels permeable to Na^+ open, some Na^+ enters the fiber, and the membrane potential swings transiently toward E_{Na}. When these pores close again, the membrane potential returns to rest near E_K and E_{Cl}. During activity the extra ion fluxes impose an extra load on the Na^+/K^+ pump and the Ca^{2+} pump, consuming ATP and stimulating an extra burst of cellular oxygen consumption until the original gradients are restored.

How large are these fluxes? The physical minimum, calculated from the rules of electricity, is very small. Only 10^{-12} equivalents of charge need be moved to polarize 1 cm^2 of membrane by 100 mV, meaning that, ideally, the movement of 1 pmol/cm^2 of monovalent ion would be enough to depolarize the membrane fully. With this kind of Na^+ gain, a squid giant axon of 1 mm diameter could be stimulated 10^5 times and a mammalian unmyelinated fiber of 0.2 μm diameter only 10–15 times before the internal Na^+ concentration would be doubled, assuming that the Na, K pump had been blocked.

Gating mechanisms for Na^+ and K^+ channels in the axolemma are voltage dependent

The breakthrough in explaining the action potential came with an electrical method to study the kinetics of ion permeability changes directly. In a classic series of experiments, Hodgkin, Huxley and Katz (Hodgkin, 1964; Nicholls et al., 2001; Hille, 1997, 2001; Hodgkin & Huxley, 1952) studied squid giant-axon membranes by the method they called the voltage clamp. Their method controls the membrane voltage electrically while ion movements are recorded as electric current flowing across the membrane. The recorded current can be resolved into individual ionic components by changing the ion content of the solutions that bathe the membrane. The voltage clamp is a rapid and sensitive assay for studying the opening and closing of ion channels. Today, a widely used miniature version of the voltage clamp is the patch clamp, which has sufficient sensitivity to study the current flow in a single ion channel (Hamill et al., 1981). A glass micropipette, the patch pipette, with a tip diameter <1 μm, is fire polished at the tip and then pressed against the membrane of a cell. Because the tip is smooth, it seals to the membrane in the annular contact zone, rather than piercing the membrane, and defines a tiny patch of the cell surface whose few ion channels can be detected easily by the currents flowing through them. The patch clamp readily measures fluxes of as little as 10^{-20} mol of ion in less than 1 ms.

With the voltage clamp, Hodgkin and Huxley (Hodgkin, 1964; Hodgkin et al., 1952; Bezanilla, 2000) discovered that the opening and closing conformational changes of axonal Na^+ and K^+ channels are directly controlled by the membrane potential. Hence, channel gating (these conformational changes) derives its energy from the work done by the electric field on charged residues of the channel macromolecule. Hodgkin and Huxley (1952) identified currents from two types of ion-selective channel—Na^+ channels and K^+ channels—that account for almost all the current in axon membranes. Then they made a kinetic model of the opening and closing steps, simplified in Figure 4-3. Depolarization of the membrane is sensed by the voltage sensors of each channel and causes the conformational reactions to proceed to the right. Repolarization or hyperpolarization causes them to proceed to the left. We can understand the action potential in these terms. The action potential, initiated by a depolarizing stimulus, begins with a transient, voltage-gated opening of Na^+ channels that allows Na^+ to enter the fiber and depolarize the membrane fully, followed by a transient, voltage-gated opening of K^+ channels that allows K^+ to leave and repolarize the membrane. Figure 4-4 shows a calculation of the temporal relation between channel-opening and membrane-potential changes in an axon at 18.5°C, using the full kinetic model of Hodgkin & Huxley (1952).

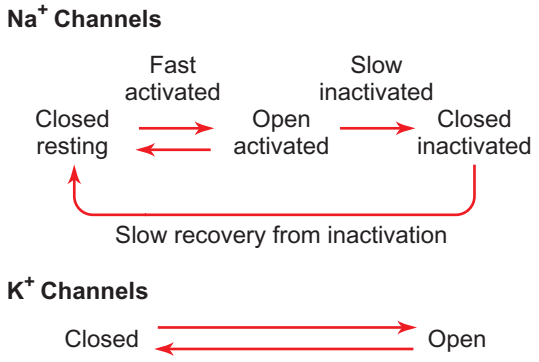

FIGURE 4-3 **Simplified kinetic model for opening and closing steps of Na^+ and K^+ channels.** Adapted from Hodgkin & Huxley (1952).

The action potential is propagated by local spread of depolarization

How does the action potential propagate smoothly down an axon, bringing new channels into play ahead of it? Any electrical depolarization or hyperpolarization of a cell membrane spreads a small distance in either direction from its source by a purely passive process often called cable spread or electrotonic spread. The spread occurs because the intracellular and extracellular media are much better conductors than is the membrane, so that any charges injected at one point across the membrane repel each other and disperse along the membrane surface. The lower part of Figure 4-4 shows diagrammatically the so-called local circuit currents that spread the depolarization forward. In this way, an excited depolarized membrane area smoothly depolarizes the next unexcited region ahead of the action potential, bringing it above firing threshold, opening Na^+ channels there, and advancing the wave of excitation. The action potential in the upper part of Figure 4-4 is calculated by combining the known geometry of the squid giant axon with the rules of ionic electricity and the Hodgkin and Huxley kinetic equations for the voltage-dependent gating of Na^+ and K^+ channels. The success of the calculations means that the factors described are sufficient to account for action-potential propagation, a triumph of biophysics.

Membranes at nodes of ranvier have high concentrations of Na^+ channels

A wide variety of cells have now been studied by voltage clamp methods, and quantitative descriptions of their permeability changes are available. All axons, whether vertebrate or invertebrate, operate on the same principles: They have a small background permeability, primarily to K^+, that sets the resting potential and display brief, dramatic openings of Na^+ and K^+ channels in sequence to shape the action potentials. Chapter 10 describes myelin, a special adaptation of large (1–20 μm diameter) vertebrate nerve fibers for higher conduction speed. In myelinated nerves, like unmyelinated ones, the depolarization spreads from one excitable membrane patch to another by local circuit currents; but, because of the insulating

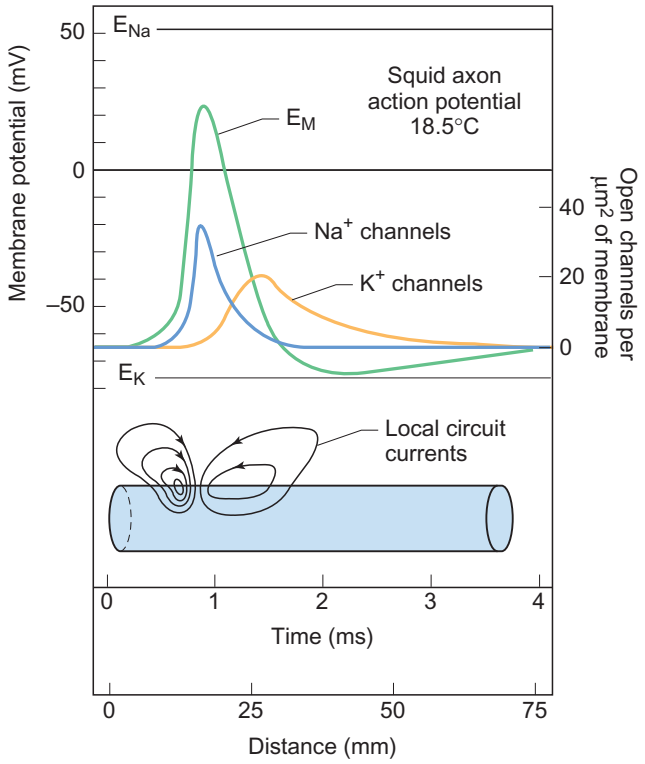

FIGURE 4-4 **Events of the propagated action potential calculated from the Hodgkin & Huxley (1952) kinetic model.** Because the action potential is a nondecrementing wave, the diagram shows equivalently the time course of events at one point in the axon or the spatial distribution of events at one time as the excitation propagates to the left. **Upper.** Action potential (E_M) and the opening and closing of Na^+ and K^+ channels. The Nernst potentials for Na^+ and K^+ are indicated by E_{Na} and E_K. **Lower.** Local circuit currents. The intense loop on the left spreads the depolarization to the left into the unexcited membrane.

properties of the coating myelin, the excitable patches of axon membrane (the nodes of Ranvier) may be more than 1 mm apart, so the rate of progression of the impulse is faster. Nodes of Ranvier have at least 10 times as many Na^+ channels per unit area as other axons to depolarize the long, passive internodal myelin. The Na^+/K^+ pump is also concentrated at nodes (see Ch. 3). Between nodes, the internodal axon membrane has K^+ channels but far fewer Na^+ channels.

FUNCTIONAL PROPERTIES OF VOLTAGE-GATED ION CHANNELS

Ion channels are macromolecular complexes that form aqueous pores in the lipid membrane

We have learned much about ion channel function from voltage clamp and patch clamp studies on channels still imbedded in native cell membranes (Hodgkin, 1964; Armstrong, 2003; Nicholls et al., 2001; Hille, 1997, 2001; Hodgkin & Huxley, 1952; Bezanilla, 2000). A diversity of channel types was discovered in the different cells in the body, where the repertoire of

functioning channels is adapted to the special roles each cell plays (Hille, 2001). The principal voltage-gated ones are the Na^+, K^+ and Ca^{2+} channels, and most of these are opened by membrane depolarizations. Figure 4-5A summarizes the major functional properties of a voltage-gated channel in terms of a fanciful cartoon drawn before the availability of crystal structures. The pore is narrow enough in one place, the ionic selectivity filter, to 'feel' each ion and to distinguish among Na^+, K^+, Ca^{2+} and Cl^-. The channel also contains charged components that sense the electric field in the membrane and drive conformational changes that open and close gates controlling the permeability of the pore. In voltage-gated Na^+, K^+ and Ca^{2+} channels, the gates close the intracellular mouth of the pore and the selectivity filter is near the outer end of the pore.

How did the voltage clamp show that a channel is a pore? The most convincing evidence was the large ion flux a single channel can handle. In patch-clamp studies, it is common to observe ionic currents of 2–10 pA flowing each time one channel in the patch is open. This would correspond to 12–60 $\times$ 10^6 monovalent ions moving per second. Such a turnover number is several orders of magnitude faster than known carrier mechanisms and agrees well with the theoretical properties of a pore of atomic dimensions.

Water molecules break and make hydrogen bonds with other waters 10^{11}–10^{12} times per second, and alkali ions exchange water molecules or other oxygen ligands at least 10^9 times per second. In these terms, the progress of an ion across the membrane is not the movement of a fixed hydrated complex; rather, it is a continual exchange of oxygen ligands as the ion dances through the sea of relatively free water molecules and polar groups that form the wall of the pore. Dipoles and charged groups in the pore provide stabilization energy to the permeating ion, compensating for those water molecules that must be left behind as the ion enters into the pore. Evidence for important negative charges in the selectivity filter of Na^+ and Ca^{2+} channels comes from a block of their permeability as the pH of the external medium is lowered below pH 5.5 (Hille, 2001) and from site-directed mutagenesis of aspartate and glutamate residues in cloned channels (Heinemann et al., 1992).

The minimum pore size of ion channels was first determined from the van der Waals dimensions of ions that will pass through them (Hille, 2001). The voltage-gated channels, which show considerable ion selectivity, are so narrow that ions need to shed several (not all) water molecules to pass through. The ion fluxes are often described by models with temporary binding to attractive sites and jumps over energy barriers. Formally, the kinetics of flux through channels can be formulated similarly to enzyme kinetics. It is assumed that the channel passes through a sequence of 'channel–ion complexes' as it catalyzes the progression of an ion across the membrane. Such theories also can describe other properties of ion channels, such as selectivity, saturation, competition and block by permeant ions (Hille, 2001).

Voltage-dependent gating requires voltage-dependent conformational changes in the protein component(s) of ion channels

On theoretical grounds, a membrane protein that responds to a change in membrane potential must have charged or dipolar amino acid residues, located within the membrane electric field, acting as voltage sensors as illustrated in Figure 4-5A (Hille, 2001; Hodgkin & Huxley, 1952; Bezanilla, 2000). Changes in the membrane potential then exert a force on these charged residues. If the energy of the field-charge interactions is great enough, the protein may be induced to undergo a change to a new, stable conformational state in which the net charge or the location of charge within the membrane electric field has been altered. For such a voltage-driven change of state, the steepness of the state function versus membrane potential curve defines the equivalent number of charges that move, according to a Boltzmann distribution. On this basis, activation of Na^+ channels would require the movement of as many as 12 positive charges from the intracellular to the extracellular side of the membrane. The movement of a larger number of charges through a proportionately smaller fraction of the membrane electrical field would be equivalent.

Such movements of membrane-bound charge give rise to tiny 'gating' currents that can be detected electrophysiologically (Armstrong, 1981). Their voltage and time dependence are consistent with the multistep changes of channel state from resting to active. In contrast to activation, fast inactivation from the open state of Na^+ channels and certain K^+ channels does not seem to be a strongly voltage-sensitive process. This inactivation can be removed irreversibly by proteolytic enzymes acting from the intracellular side of the channel. It requires regions of the channel that are exposed at the intracellular surface of the membrane.

Pharmacological agents acting on ion channels help define their functions

The Na^+ channel is so essential to successful body function that it has become the target in evolution of several potent poisons. The pharmacology of these agents has provided important insights into the further definition of functional regions of the channel (Armstrong, 2003; Hille, 2001; Catterall, 1980). Figure 4-5B shows the probable sites of action of four prominent classes of Na^+ channel agents. At the outer end of the channel pore is a site where the puffer fish poison tetrodotoxin (TTX), a small, lipid-insoluble charged, binds with a K_i of 1–10 nmol/l and blocks Na^+ permeability. A second important class of Na^+ channel blockers includes such clinically useful local anesthetics as lidocaine and procaine and related antiarrhythmic agents. They are lipid-soluble amines with a hydrophobic end and a polar end, and they bind to a hydrophobic site on the channel protein where they also interact with the inactivation gating machinery. The relevant clinical actions of local anesthetics are fully explained by their mode of blocking Na^+ channels. Two other classes of toxins either open Na^+ channels spontaneously or prevent them from closing normally once they have opened. These are lipid-soluble steroids, such as the frog-skin poison batrachotoxin (BTX) and the plant alkaloids aconitine and veratridine, all three of which act at a site within the membrane, and peptide toxins from scorpion and anemone venoms, which act at two sites on the outer surface of the membrane. Most scorpion and anemone toxins block the inactivation gating step specifically. Interestingly, the affinity of the channel for each of these classes of toxins depends on the gating conformational state of the channel.

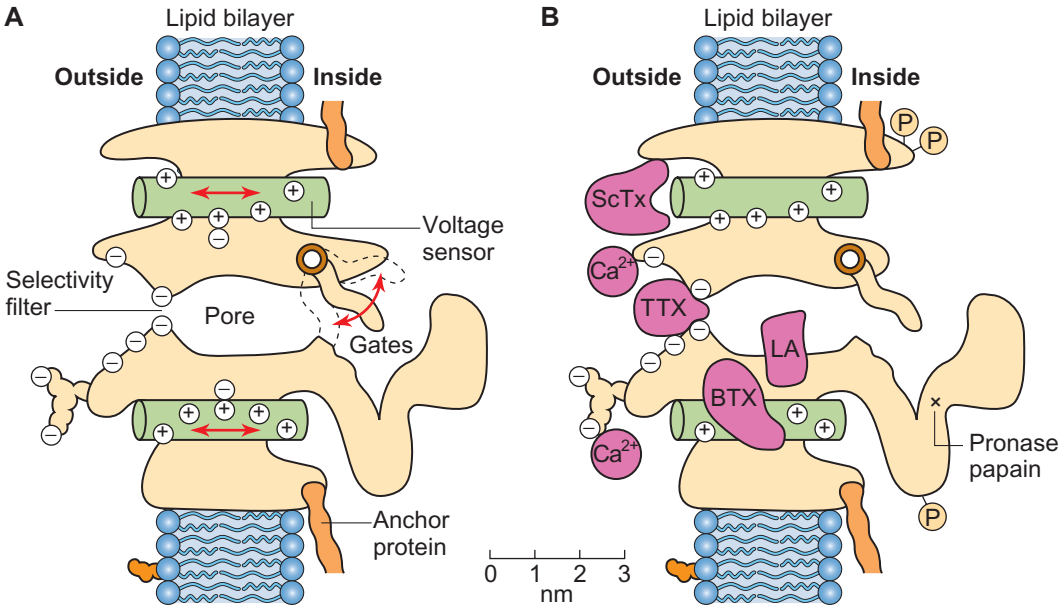

FIGURE 4-5 **(A) Diagram of the functional units of a voltage-gated ion channel and (B) the hypothesized binding sites for several drugs and toxins affecting Na^+ channels.** The drawing is fanciful, and the dimension and shapes of many parts are not known. Drug receptors: *TTX*, tetrodotoxin and saxitoxin; *ScTx*, scorpion toxins and anemone toxins; *BTX*, batrachotoxin, aconitine, veratridine and grayanotoxin; *LA*, local anesthetics; *Ca^{2+}*, divalent ions screening and associating with surface negative charge.

Similarly, specific agents affect K^+ channels or Ca^{2+} channels. Most K^+ channels can be blocked by tetraethylammonium ion, Cs^+, Ba^{2+} and 4-aminopyridine (Armstrong, 2003; Hille, 2001). Except for 4-aminopyridine, there is good evidence that these ions become lodged within the channel at a narrow place from which they may be dislodged by K^+ coming from the other side. In addition, certain K^+ channels can be distinguished by their ability to be blocked near the outer mouth by polypeptide toxins from scorpion (charybdotoxin), bee (apamin), or snake (dendrotoxin) venoms. Ca^{2+} channels can be blocked by externally applied divalent ions, including Mn^{2+}, Co^{2+}, Cd^{2+} and Ni^{2+}. Different Ca^{2+} channel subtypes can be distinguished by their block by dihydropyridines (nifedipine), cone snail toxins (ω-conotoxins) and spider toxins (agatoxins).

THE VOLTAGE-GATED ION CHANNEL SUPERFAMILY

Why should we study the structural properties of the channel macromolecules themselves? Although biophysical techniques define the functional properties of voltage-sensitive ion channels clearly, it is important to relate those functional properties to the structure of the channel proteins. We focus first on the discovery of the ion channel proteins, in which three different experimental approaches were used.

Na^+ channels were identified by neurotoxin labeling and their primary structures were established by cDNA cloning

Neurotoxins act at several different sites on Na^+ channels to modify their properties (Figures 4-5B, 4-6A). Photoreactive derivatives of the polypeptide toxins of scorpion venom were covalently attached to Na^+ channels in intact cell membranes, allowing direct identification of channel components. Reversible binding of saxitoxin and tetrodotoxin to their common receptor was used as a biochemical assay for the channel protein. Solubilization of excitable membranes with nonionic detergents released the Na^+ channel, and the solubilized channel was purified by chromatographic techniques that separate glycoproteins by size, charge and composition of covalently attached carbohydrate (Agnew, 1984; Barchi, 1984; Catterall, 1986). Na^+ channels consist of a large α-subunit, a glycoprotein with molecular mass of 260,000, that is usually in association with glycoprotein β-subunits with molecular masses of 33,000–36,000 (Fig. 4-6A). An important step in the study of a purified membrane transport protein is to reconstitute its function in the pure state. This was accomplished by reconstitution of the Na^+ channel in phospholipid vesicles and in planar phospholipid bilayers. The purified channels retained the voltage dependence, ion selectivity, and pharmacological properties of native channels, confirming that the correct ion channel protein had been purified in functional form.

The amino acid sequences of the Na^+ channel α, β1 and β2 subunits were determined by cloning and sequencing DNA complementary to their mRNAs, using antibodies protein sequence, and oligonucleotides developed from work on purified Na^+ channels (Noda et al., 1986; Isom et al., 1994; Catterall, 2000a). The primary structures of these subunits are illustrated as transmembrane folding models in Figure 4-6B. The large α subunits are composed of 1,800–2,000 amino acids and contain four repeated domains having greater than 50% internal sequence identity. Each domain contains six segments that form transmembrane α-helices and an additional membrane reentrant loop that forms the outer mouth of the

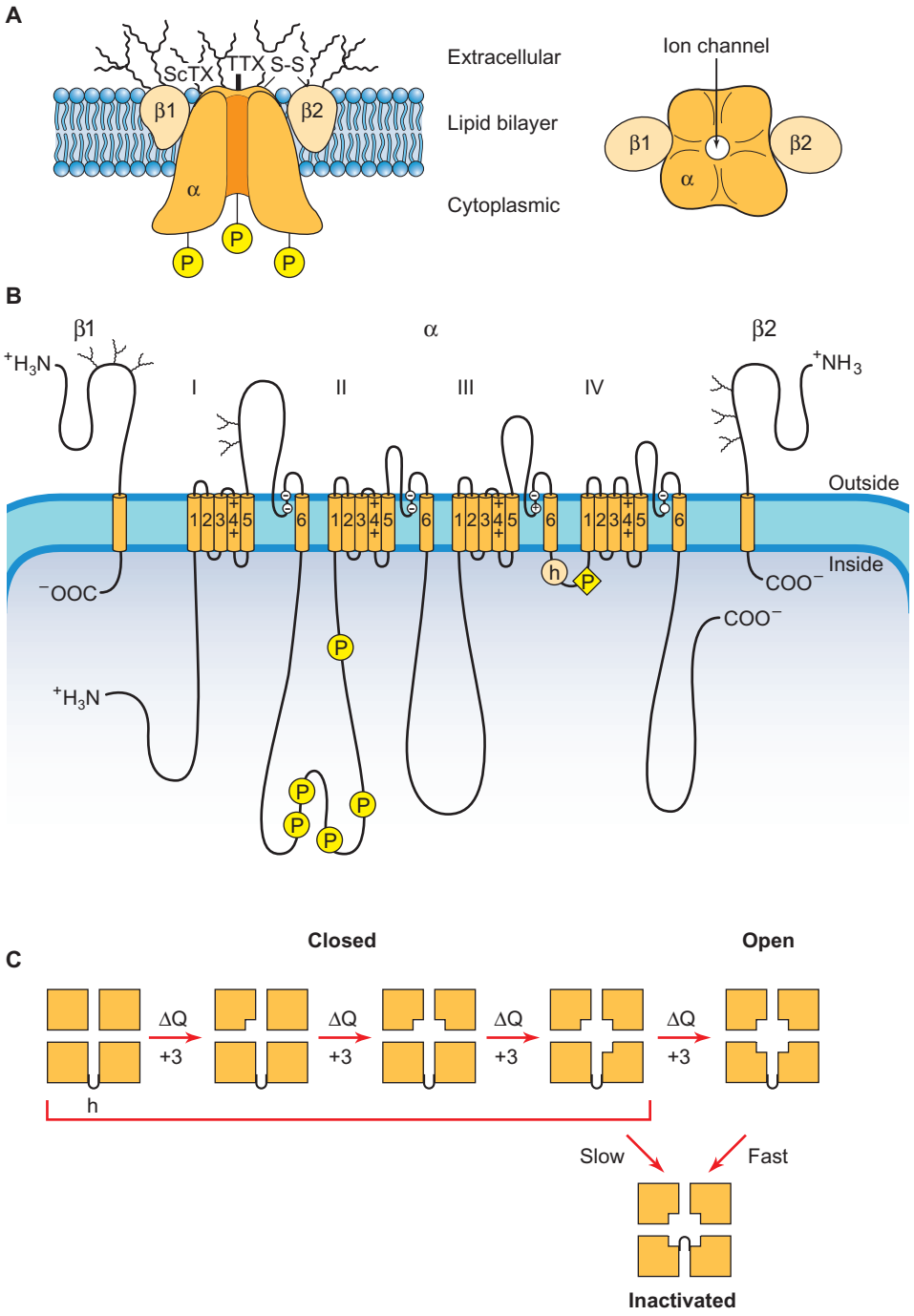

FIGURE 4-6 **Structural model of the Na^+ channel. (A) Left.** A topological model of the rat brain Na^+ channel illustrating the probable transmembrane orientation of the three subunits, the binding sites for tetrodotoxin (*TTX*) and scorpion toxin (*ScTX*), oligosaccharide chains *(wavy lines)* and cAMP-dependent phosphorylation sites (*P*). **Right.** An *en face* view of the protein from the extracellular side illustrating the formation of a transmembrane ion pore in the midst of a square array of four transmembrane domains of the α subunit. **(B)** A transmembrane folding model of the α and β subunits of the Na^+ channel. The amino acid sequence is illustrated as a *narrow line*, with each segment approximately proportional to its length in the molecule. Transmembrane α-helices are illustrated as cylinders. The positions of amino acids required for specific functions of Na^+ channels are indicated: + + positively charged voltage sensors in the S4 transmembrane segments; *O*, residues required for high affinity binding of TTX with their charge characteristics indicated by −, + or open field; *h*, residues required for fast inactivation; *P in a circle*, sites for phosphorylation by cAMP-dependent protein kinase; and *P in a diamond*, sites for phosphorylation by protein kinase C. **(C)** Sequential gating of the Na^+ channel. A reaction pathway from closed to open Na^+ channels is depicted. Each square represents one homologous domain of the α subunit. Each domain undergoes a conformational change initiated by a voltage-driven movement of its S4 segment, leading eventually to an open channel. Inactivation of the channel occurs from the final closed state and the open state by folding of the intracellular loop connecting domains III and IV into the intracellular mouth of the transmembrane pore.

transmembrane pore (see below). In contrast, the smaller β1 and β2 subunits consist of a large extracellular N-terminal segment with a structure similar to antigen-binding regions of immunoglobulin, a single transmembrane segment and a short intracellular segment (Fig. 4-6B).

Ca^{2+} channels have a structure similar to Na^+ channels

The same general experimental strategy was successfully applied to voltage-gated Ca^{2+} channels. Drugs and neurotoxins that act on Ca^{2+} channels were used to identify and purify their protein components, and the ion transport function of the purified channels was restored by reconstitution (Fig. 4-7A) (Catterall, 2000b; Hofmann et al., 1994). Like Na^+ channels, Ca^{2+} channels have a principal subunit, designated α1, which is structurally homologous to the Na^+ channel α subunit. They have associated α2 and δ subunits, which form a disulfide-linked transmembrane glycoprotein complex, and β subunits, which are intracellular (Fig. 4-7A). In addition, Ca^{2+} channels in skeletal muscle have a transmembrane γ subunit. The auxiliary subunits of Ca^{2+} channels are not related in primary structure to the Na^+ channel β subunits.

Voltage-gated K^+ channels were identified by genetic means

Genes that harbor mutations causing an easily detectable altered phenotype can be cloned directly from genomic DNA without information about the protein they encode. The *Shaker* mutation in *Drosophila* causes flies to shake when under ether anesthesia and is accompanied by loss of a specific K^+ current in the nerve and muscle of the mutant flies. Cloning successive pieces of genomic DNA from the region of the chromosome that specifies this mutation allowed isolation of DNA clones encoding a protein related in amino acid sequence to the α subunit of Na^+ channels (Jan & Jan, 1997). The K^+ channel protein is analogous to one of the homologous domains of Na^+ or Ca^{2+} channels (Jan & Jan, 1997) and functions as a tetramer of four separate subunits, analogous to the structure of Na^+ and Ca^{2+} channels (Fig. 4-7B). Like the Na^+ channels and the Ca^{2+} channels, the K^+ channels have auxiliary subunits, which include intracellularly located β subunits as well as minK or minK-related subunits that have a single transmembrane segment (Jan & Jan, 1997; Pongs, 1999).

Inwardly rectifying K^+ channels were cloned by expression methods

A third experimental approach was used to clone and characterize inwardly rectifying K^+ channels, the simplest member of the ion channel protein family (Jan & Jan, 1997; Doupnik et al., 1995). DNA complementary to mRNAs from brain or heart was prepared and separated into pools. mRNA was prepared from each pool and its ability to direct the synthesis of K^+ channels in *Xenopus* oocytes was measured. The active cDNA was isolated by repeatedly dividing the pool of cDNAs until only a single one remained. The amino acid sequence that it encoded showed that inwardly rectifying K^+ channels have only two transmembrane segments (Fig. 4-7B), analogous to the S5 and S6 segments of voltage-gated Na^+, Ca^{2+} or K^+ channels. Four subunits are required to form an ion channel. Thus, these two segments also form the transmembrane pores of voltage-gated Na^+, Ca^{2+} or K^+ channels.

THE MOLECULAR BASIS FOR ION CHANNEL FUNCTION

The cloning of the cDNA encoding the ion channel subunits permitted detailed tests of the functional properties of the polypeptides. cDNA clones can be expressed in recipient cells and the resulting ion channels can be studied by voltage-clamp methods. Only the principal α subunits of the Na^+, Ca^{2+} or K^+ channels are required for function (Noda et al., 1986; Goldin et al., 1986). However, co-expression of the auxiliary subunits increases the level of expression and modifies the voltage-dependent gating, conferring more physiologically correct functional properties on the expressed channels (Isom et al., 1994). These results indicate that the principal subunits of the voltage-gated ion channels are functionally autonomous, but the auxiliary subunits improve expression and localization and modulate physiological properties.

Much is known about the structural determinants of the ion selectivity filter and pore

Which amino acid sequences are involved in forming the ion selectivity filter and pore? Insight into this question first came from studies of the amino acid residues required for binding of tetrodotoxin, which blocks the Na^+ channel ion selectivity filter at the outer mouth of the pore (Fig. 4-5B). Site-directed mutagenesis experiments showed that pairs of amino acid residues required for high-affinity tetrodotoxin binding are located in analogous positions in all four domains near the carboxyl ends of the short membrane-re-entrant segments between transmembrane α-helices S5 and S6 (Terlau et al., 1991) (Fig. 4-6B). Six of these eight residues are negatively charged and may interact with permeant ions as they approach and move through the channel. In agreement with this idea, mutation of the only two of these residues that are not negatively charged (see domains III and IV, Fig. 4-6B) to glutamic acid residues, as present in the analogous positions in the Ca^{2+} channel, confers Ca^{2+} selectivity on the Na^+ channel (Heinemann et al., 1992). Parallel results implicated these same regions of the K^+ channel in determining ion selectivity and conductance (Miller, 1990). These results led to the idea that these segments, often called the P loops, form the ion selectivity filter. The three-dimensional structure of the pore formed from the S5 and S6 segments and the intervening P loop was elegantly determined by X-ray crystallography of a bacterial K^+ channel (Doyle et al., 1998). As in inward rectifier K^+ channels (Fig. 4-7B), the subunits of this bacterial channel have just two transmembrane segments (analogous to S5 and S6), which form α-helices that cross the membrane at an

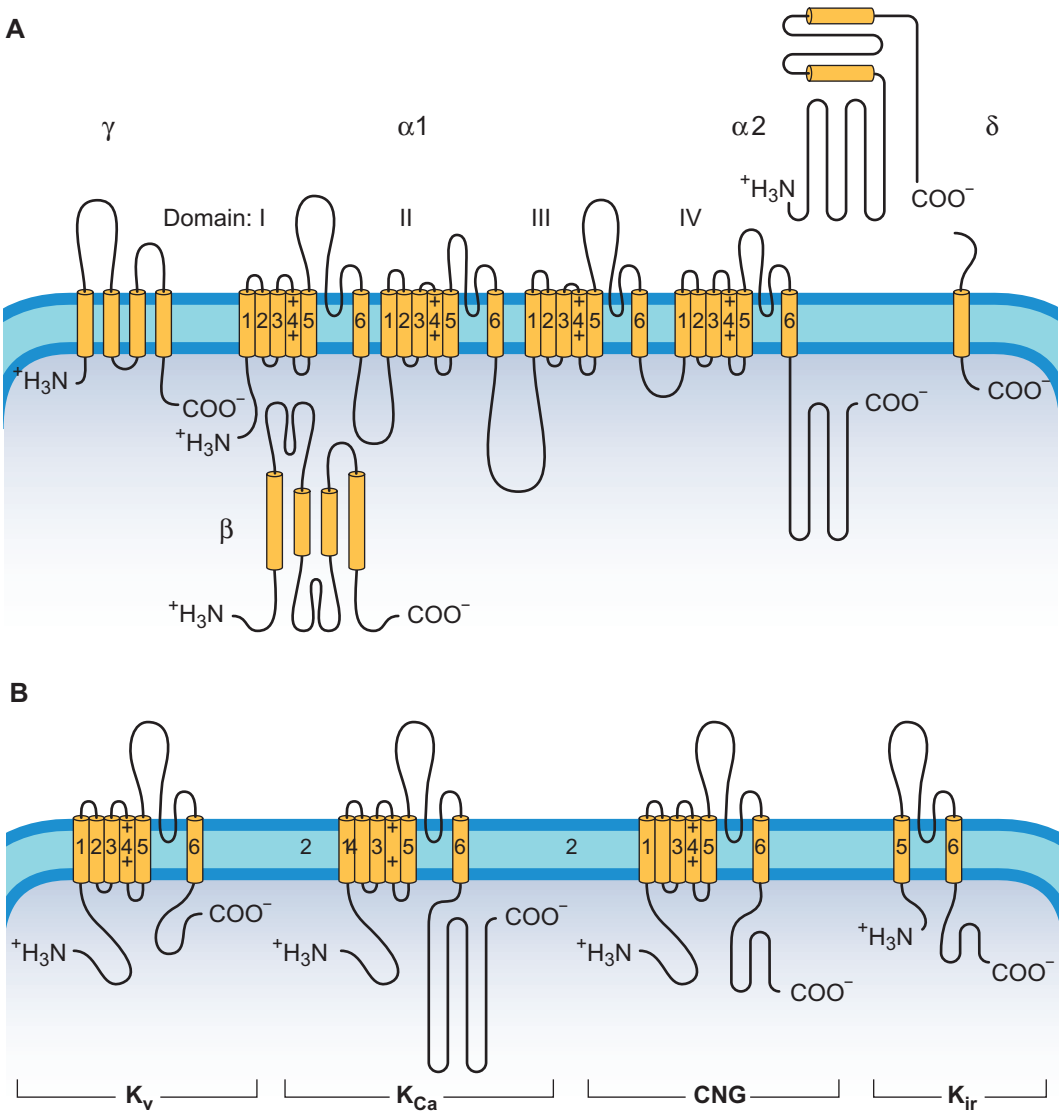

FIGURE 4-7 **Transmembrane organization of voltage-gated Ca^{2+} channels, K^+ channels and relatives. (A)** The primary structures of the subunits of voltage-gated Ca^{2+} channels are illustrated. *Cylinders* represent probable α-helical transmembrane segments. *Bold lines* represent the polypeptide chains of each subunit, with length approximately proportional to the number of amino acid residues. **(B)** The primary structures of the plasma membrane cation channels related to K^+ channels are illustrated as transmembrane folding diagrams based on analysis of the hydrophobicity of the amino acid sequence. Transmembrane α-helices are illustrated as *cylinders*. The remainder of the polypeptide chain is illustrated as a *bold line*, with the length of each segment approximately proportional to the length of its amino acid sequence. K_V, voltage-gated K^+ channel; K_{Ca}, Ca^{2+}-activated K^+ channel types 2 and 3; *CNG*, cyclic nucleotide-gated channel; K_{ir}, inward rectifying K^+ channel.

angle to form an 'inverted teepee' structure (Fig. 4-8A, left). The P loops are cradled in this structure to form the narrow ion selectivity filter at the extracellular end of the pore. This remarkable structure elucidates the molecular basis for the formation of a transmembrane pore and suggests a mechanism for ion conduction (see below).

How does the pore open? The structure illustrated in Figure 4-8A (left) may represent the closed state because the α-helices lining the inner pore cross at their intracellular ends, apparently closing the pore. In contrast, the structure of a distantly related bacterial K^+ channel (Jiang et al., 2002), which is gated open by binding of Ca^{2+}, has a bend of approximately 30° in the inner pore helix (analogous to S6) at the position of a highly conserved glycine residue (Fig. 4-8A, right). This conformational change appears to open the pore at its intracellular end by splaying open the bundle of inner pore helices. Mutational studies of Na^+ channels support this pore-opening model because replacement of the conserved glycine with proline, which strongly favors a bend in the α-helix, also strongly favors pore opening and greatly slows closure (Zhao et al., 2004).

Once the pore is open, K^+ ions appear to move outward in single file. Analysis of crystals shows that four K^+ ions can interact with the backbone carbonyl groups of the amino acid residues that form the ion selectivity filter (Fig. 4-8B).

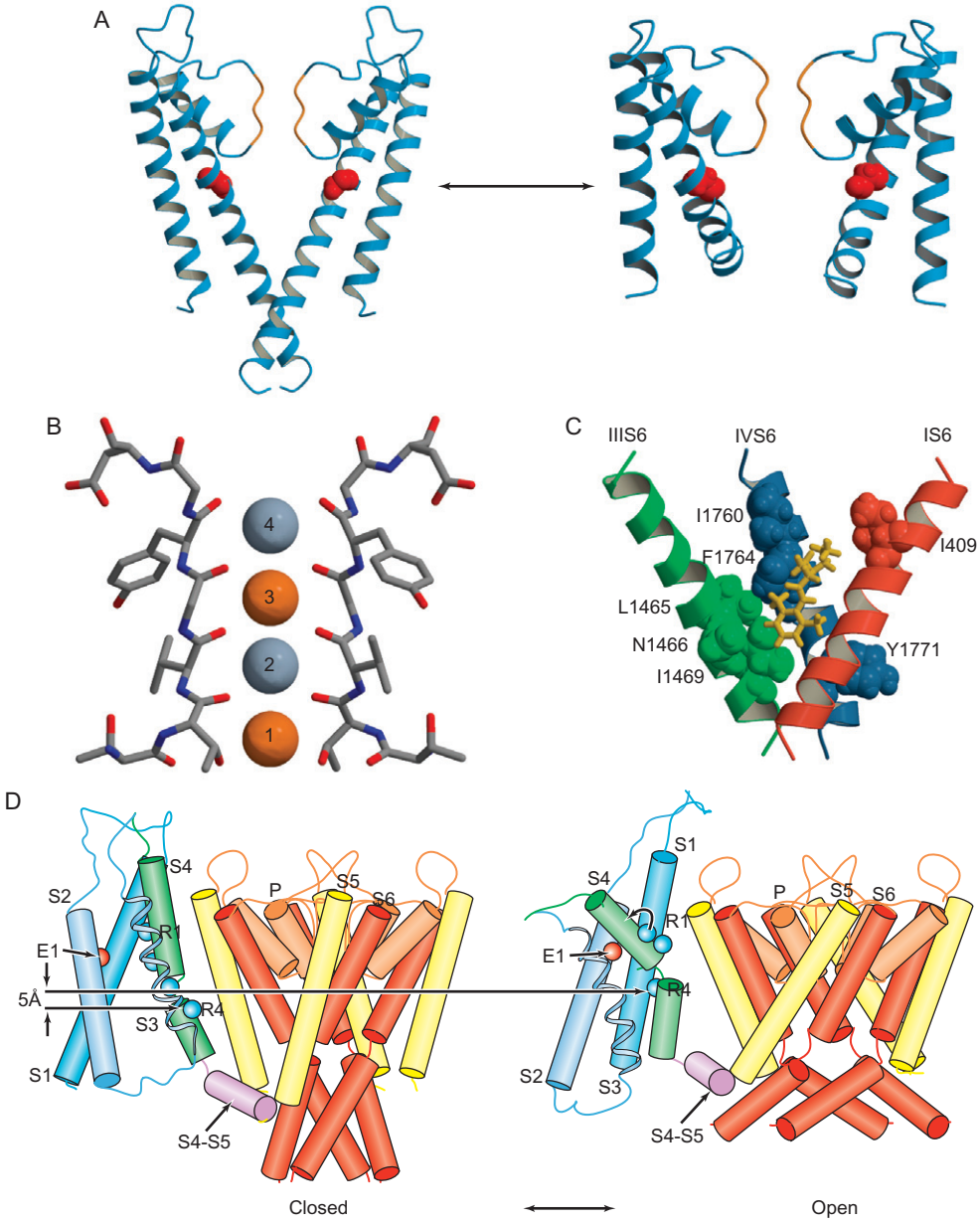

FIGURE 4-8 **The ion selectivity filter and pore of Na^+ and K^+ channel illustrated with the extracellular side upwards. (A)** A drawing of the three-dimensional structures of K^+ channels in the closed and open states, adapted from the three-dimensional structures of the K^+ channel from the bacteria *Streptococcus lividans* (closed, left) and *Methanobacterium terrmoautotrophicum* (open, right). Only two subunits are shown for clarity. **(B)** A drawing of K^+ ions moving single file through the ion selectivity filter of the K^+ channel from *S. lividans*. The four ion-coordination sites are thought to work in pairs. In one cycle of outward K^+ conductance, K^+ ions occupy sites 1 and 3 (orange), shift to sites 2 and 4 (gray), and then the K^+ ion in site 4 moves into the extracellular space while a new K^+ ion occupies site 1 and the K^+ ion in site 2 moves to site 3, reestablishing the initial state. **(C)** A drawing of the local anesthetic receptor site in the pore of the Na^+ channel. The amino acid residues that are thought to contact a bound etidocaine molecule (yellow) are indicated in a space-filling format for the S6 segments in domains I (red), III (green) and IV (blue). **(D)** The structure of a K_V channel in resting and activated/open states. The structure of the voltage-gated K^+ channel $K_V1.2$ is illustrated as a molecular model derived from X-ray crystallographic determination of the structure of the activated state of the channel (Long et al., 2005) and modeling of the testing state (Yarov-Yarovoy et al., 2006. The figure illustrates a complete pore formed from the S5 (yellow) and S6 (red) transmembrane segments plus the P loop between them (orange) from four subunits of the channel. For clarity, only a single voltage sensor from one subunit of the channel is illustrated with its four transmembrane segments. Three additional voltage sensors would be symmetrically located to the right of the pore, behind it, and in front of it. The S4 segment of the voltage sensor is illustrated in green with the four positively charged arginine residues (R1-R4) that serve as gating charges superimposed as blue balls. The S1 (purple) and S2 (light blue) segments are illustrated as cylinders, and a key negatively charged residue in the S2 segment (E1) is represented as a red ball. Left, closed state. This model of the closed state is derived from structural modeling (Yarov-Yarovoy et al., 2006). Its pore is closed by the straight conformation of the S6 helices, and its S4 segment is drawn inward such that the R1 gating charge is interacting with the key negatively charged residue E1. In this inward position, the S4 segment pushes on the pore and keeps the S6 segments straight, thereby keeping the pore closed. Right, activated/open state. The model of this state of the channel is derived directly from the X-ray crystal structure (Yarov-Yarovoy et al., 2006). The intracellular end of the pore is opened by the bending of the S6 segments, as in Figure 4-8A. A unique feature of this structure is the connection of the voltage sensor on the left to the pore-forming module that is in the front of the pore through the S4-S5 linker (purple). Surprisingly, the voltage sensor makes its most intimate contacts with the pore-forming module of the adjacent subunit in clockwise direction as viewed from the extracellular side of the membrane. It is possible that this interwoven arrangement of the four subunits allows them to gate the pore simultaneously.

It is thought that two K^+ ions occupy sites 1 and 3 (Fig. 4-8B, orange) and then switch to sites 2 and 4 (gray). The K^+ ion in site 4 would dissociate into the extracellular space, the K^+ ion in site 2 would move to site 3, and another K^+ ion from the intracellular space would bind to site 1. In this way, the pore would remain occupied by two ions, during steady outward conduction.

Local anesthetics bind in the inner pore of Na^+ channels and block them (Fig. 4-5B). What is the structure of the local anesthetic binding site? A combination of site-directed mutagenesis and molecular modeling (Catterall, 2000a) reveals that local anesthetics and related antiepileptic drugs bind to a receptor formed by amino acid residues at specific positions in the S6 segments in domains I, III and IV of the Na^+ channel, as illustrated in Figure 4-8C. The aromatic and hydrophobic side chains of these amino acids contact the aromatic and substituted amino groups of the drug molecules and hold them in the receptor site, where they block ion movement through the pore.

Voltage-dependent activation requires moving charges

Structural models for voltage-dependent gating of ion channels must identify the voltage-sensors or gating charges (Fig. 4-5A) within the channel structure and suggest a plausible mechanism for transmembrane movement of gating charge and its coupling to the opening of a transmembrane pore. The S4 segments of the homologous domains have been proposed as voltage sensors (Catterall, 1986; Guy & Conti, 1990). These segments, which are conserved among Na^+, Ca^{2+} and K^+ channels, consist of repeated triplets of two hydrophobic amino acids followed by a positively charged residue. In the α-helical configuration, these segments would form a spiral of positive charge across the membrane, a structure that is well suited for transmembrane movement of gating charge (Fig. 4-5A). The positive charges are thought to be neutralized by negative charges in the nearby S2 and S3 segments. Much direct evidence in favor of designating the S4 segments as voltage sensors comes from mutagenesis studies (Bezanilla, 2000; Jan & Jan, 1997; Stühmer et al., 1989). Neutralization of positive charges results in progressive reduction of the steepness of voltage-dependent gating and of the apparent gating charge, as expected if indeed the S4 segments are the voltage sensors. At the resting membrane potential, the force of the electric field would pull the positive charges inward. Depolarization would abolish this force and allow an outward movement of the S4 helix. This outward movement has been detected in clever experiments that measure the movement of chemically reactive cysteine residues substituted for the native amino acids in S4 by analyzing the functional effects of specific chemical reactions at those substituted cysteines or the fluorescence of chemical probes located there (Bezanilla, 2000; Yang et al., 1996; Gandhi & Isacoff, 2002). This movement of the S4 helix is proposed to initiate a more general conformational change in each domain. After conformational changes have occurred in all four domains, the transmembrane pore can open and conduct ions (Fig. 4-6C).

Recent structural studies reveal the conformation of the voltage sensor. The structure of a voltage-gated K^+ channel ($K_v1.2$), determined by x-ray crystallography, reveals that the S1-S4 segments form a compact four-helix transmembrane bundle (Fig. 4-8D). The structure determined by X-ray crystallography captured the activated state of the voltage sensor and the open state of the pore. Molecular modeling methods have been used to predict the structure of the resting state (Fig. 4-8D). By comparing the predicted structure of the resting state to the experimentally determined structure of the activated state, one can visualize the movement of the voltage sensor in response to depolarization of the membrane. The gating charges in the voltage sensor (blue balls) are in an outward position in this activated state structure, as revealed by the interactions observed between R3, R4 and the key negative charge E1. The three-dimensional structure of the resting state has not been determined by X-ray crystallography. The difficulty in determining the structure of the resting state using this technique may be caused by its voltage dependence—the resting state is only observed in an excitable cell at the resting membrane potential of −70 mV to −90 mV, and there is not an equivalent membrane potential in a protein crystal. A model of the resting state has therefore been developed using protein modeling methods, based on the structure of the activated state shown here, the structure of the closed pore of the KcsA channel (Fig. 4-8D), and molecular constraints based on widely accepted experimental results. The model illustrates the pore in a closed conformation, formed by straightening of the S6 segments, and the voltage sensor in a resting conformation. The S4 segment is retracted into the cell by at least 6 Å, and the R1 and R2 gating charges are now interacting with the key negative charge E1. This inward movement of the S4 segment of the voltage sensor moves the position of the S4-S5 linker (purple) and forces closure of the pore. The model of the resting state is approximate and will likely be revised when its structure is determined by X-ray crystallography, if that is possible.

From these two structural models, one can visualize the steps in the gating of a voltage-gated ion channel. In the closed state, the negative internal membrane potential of −70 mV to −90 mV pulls the S4 gating charges inward by electrostatic force. The inward position of the S4 segment exerts a force on the S4-S5 linker, straightens the S6 segment, and closes the pore at its inner mouth. When the cell is depolarized, the electrostatic force pulling the S4 segment is relieved. In response to the change in electrostatic force, the S4 segment moves outward with each positive gating charge interacting with the negatively charged amino acid E1 in turn to ease their movement through the voltage sensor. When the R3 and R4 gating charges reach E1, the outward force on the S4-S5 linker is sufficient to pull on the pore-forming module and bend the S6 segment, resulting in opening of the pore at its intracellular end. Once the pore is open, the fast inactivation mechanism is engaged and the inactivation gate closes. This evolving structural view is still a minimal mechanism of voltage-dependent gating of an ion channel, and many details remain to be added to this picture in future research.

The fast inactivation gate is on the inside

Shortly after opening, many voltage-gated ion channels inactivate. The inactivation process of Na^+ channels can be prevented by treatment of the intracellular surface of the channel

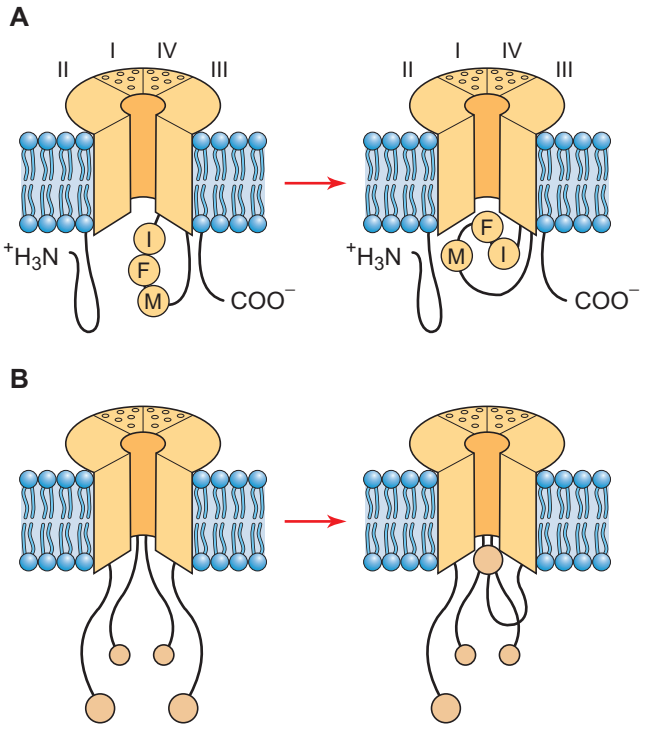

FIGURE 4-9 **Mechanisms of inactivation of Na^+ and K^+ channels. (A)** A hinged-lid model for Na^+ channel inactivation, illustrating the inactivation gate formed by the intracellular segment connecting domains III and IV and the critical cluster of hydrophobic residues that forms a latch holding the inactivation gate closed. *IFM*, isoleucine-phenylalanine-methionine. **(B)** A ball-and-chain model of K^+ channel inactivation. Each of the four subunits of a K^+ channel has a ball-and-chain structure at its N-terminus. Any one of the four can bind to the intracellular mouth of the open channel and inactivate it.

with proteolytic enzymes (Armstrong, 1981) or antibodies against the intracellular segment connecting domains III and IV (h, Fig. 4-6B) (Vassilev et al., 1998), and expression of the Na^+ channel as two pieces with a cut between domains III and IV greatly slows inactivation (Stühmer et al., 1989). A single cluster of three hydrophobic residues in this intracellular loop is required for fast inactivation (West, Patton, Scheuer et al., 1992) and inactivation is eliminated if these three hydrophobic residues are mutated to hydrophilic ones. Mutation of a single phenylalanine in the center of this motif nearly completely blocks fast inactivation of the channel. The segment of the Na^+ channel between domains III and IV is therefore proposed to serve as the inactivation gate by forming a hinged lid which folds over the intracellular mouth of the pore after activation (Catterall, 2000a) (Figs. 4-6C and 4-9A). The cluster of hydrophobic residues may bind to the intracellular mouth of the pore like a latch to keep the channel inactivated.

A detailed model of K^+ channel inactivation has been derived from mutagenesis experiments on the original *Shaker* K^+ channels from *Drosophila* (Armstrong, 2007; Hoshi et al., 1990; Zagotta et al., 1990). The N-terminal of the K^+ channel serves as an inactivation particle and both charged and hydrophobic residues are involved. A ball-and-chain mechanism (Armstrong, 1981; Hoshi et al., 1990; Zagotta et al., 1990) has been proposed in which the N-terminal segment serves as a loosely tethered ball that inactivates the channel by diffusion and binding in the intracellular mouth of the pore (Fig. 4-9B). Consistent with this mechanism, synthetic peptides whose amino acid sequences correspond to that of the inactivation particle region can restore inactivation to channel mutants whose N-terminus has been removed. The mechanisms of inactivation of Na^+ and K^+ channels are similar in that in each case hydrophobic amino acid residues seem to mediate binding of an inactivation particle to the intracellular mouth of the pore. They differ in that charged amino acid residues are important in the inactivation particle of K^+ channels but not Na^+ channels, and that the inactivation particle is located over 200 residues away from the membrane at the N-terminus of the K^+ channel, compared to only 12 residues away from the membrane between domains III and IV of the Na^+ channel. It is likely that the hinged-lid mechanism of Na^+ channel inactivation evolved from the ball-and-chain mechanism of K^+ channels.

ION CHANNEL DIVERSITY

There are a surprisingly large number of evolutionarily and structurally related ion channel proteins—in the human genome more than 140 genes encode these proteins (Table 4-2) (Hille, 2001; Catterall et al., 2002). What do they all do? Experiments in progress in many laboratories are beginning to reveal the meaning of this exceptional ion channel diversity.

Na^+ channels are primarily a single family

There are 10 human genes encoding voltage-gated Na^+ channels (Table 4-2), and at least 9 of the 10 encode members of a single family ($Na_V1.1$–1.9) (Catterall et al., 2002). These Na^+ channels are expressed in different tissues and cells, but their function is almost always to initiate action potentials in response to membrane depolarization.

Three subfamilies of Ca^{2+} channels serve distinct functions

In many cell types, it is not uncommon to find several Ca^{2+} channels that open with depolarization. The inflow of Ca^{2+} can assist in depolarizing cells, but it also performs an important messenger role. The entering Ca^{2+} may activate exocytosis (secretion), contraction, gating of other channels, ciliary reorientation, metabolic pathways, gene expression, etc. (see Ch. 24). Indeed, whenever an electrical message activates any non-electrical event, a change of the intracellular free Ca^{2+} concentration acts as an intermediary.

Genes that encode voltage-gated Ca^{2+} channels (Table 4-2) are grouped in three subfamilies that have distinct functions. In general, the members of a subfamily are greater than 75% identical in amino acid sequence in their conserved transmembrane regions, while there is only 25–50% amino acid sequence identity between these subfamilies (Catterall et al., 2002). The Ca_V1 subfamily of Ca channels conducts L-type Ca currents that initiate excitation–contraction coupling in

TABLE 4-2 The Voltage-gated Ion Channel Protein Superfamily

Channel family	Symbol	No. in human genome	Primary activators	Primary physiological roles in neurons
Voltage-gated Na^+ channel	Na_V	10	Depolarization	Initiate action potentials
Voltage-gated Ca^{2+} channel	Ca_V	10	Depolarization	Couple depolarization to Ca^{2+} entry; repetitive firing
Voltage-gated K^+ channel	K_V	40	Depolarization	Repolarization
Inwardly rectifying K^+ channels	K_{ir}	15	G protein βγ-subunits, ATP	Set and regulate resting membrane potential
Two-pore K^+ channels	K_{2P}	15	Constitutively open	Set resting membrane potential
Calcium-activated K^+ channel	K_{Ca}	8	Depolarization and Ca^{2+}	Repolarization; regulation of repetitive firing
Cyclic nucleotide-gated channels	CNG	6	Cyclic AMP and cyclic GMP	Visual and olfactory sensory transduction
Hyperpolarization and cyclic nucleotide-gated channels	HCN	4	Hyperpolarization; cyclic AMP and cyclic GMP	Regulation of firing rate and pattern; regulation of pacemaking
Transient receptor potential channels	TRP	32	Lipid messengers; heat and cold	Ca^{2+} homeostasis, thermal and pain sensation

muscle cells and secretion in endocrine cells, control gene transcription, and regulate many enzymes. The Ca_V2 subfamily conducts N-, P/Q-, and R-type Ca^{2+} currents and is particularly concentrated in nerve terminals where a Ca^{2+} influx is required for fast release of chemical neurotransmitters (see Ch. 12). The Ca_V3 subfamily conducts T-type Ca currents that are activated at negative membrane potentials and are transient. These channels are important in repetitively firing cells, like the sinoatrial nodal cells that serve as pacemakers in the heart and the neurons in the thalamus that generate sleep rhythms. This division of Ca^{2+} channels is ancient—the worm *Caenorhabditis elegans* has a single member of each of these Ca^{2+} channel subfamilies. Evidently, specialization of Ca^{2+} signaling is crucial for even simple nervous systems.

There are many families of K^+ channels

K^+ channels have many different roles in cells. For example, in neurons they terminate the action potential by repolarizing cells, set the resting membrane potential by dominating the resting membrane conductance, determine the length and frequency of bursts of action potentials, and respond to neurotransmitters by opening or closing and causing prolonged changes in membrane potential (Hille, 2001). These channels are regulated by a combination of voltage, G proteins and intracellular second messengers. Many K^+ channels are gated primarily by voltage (K_V, Table 4-2). They can be divided into 12 subfamilies based on their amino acid sequence relationships (Catterall et al., 2002). In neurons, all the K_V channels are primarily involved in repolarizing the membrane to terminate action potentials.

In addition to the K_V family, the inward rectifier family, K_{ir} (Table 4-2), comprises seven subfamilies of channels (Jan & Jan, 1997; Catterall et al., 2002) that are primarily involved in setting the resting membrane potential. The $K_{ir}3$ subfamily is strikingly activated by G protein βγ subunits released by activation of G-protein–coupled receptors (see Ch. 21). This has an important regulatory influence on the resting membrane potential in many neurons. The $K_{ir}6$ subfamily forms a complex with a large nucleotide binding protein (the sulfonylurea receptor, SUR) to form ATP-gated K^+ channels that couple changes in intracellular ATP and ADP to changes in the resting membrane potential.

A third type of K^+ channel, K_{2P}, has a structure similar to two fused K_{ir} subunits, and only two K_{2P} subunits are required to form a pore (Table 4-2) (Goldstein et al., 2001; Matulef & Zagotta, 2003). These channels are often called leak channels or open rectifiers because they are continuously open. Like the K_{ir} channels they are important in setting the resting membrane potential. Their activity is often regulated by lipid messengers or kinases.

More ion channels are related to the Na_V, Ca_V and K_V families

Remarkably, evolution has created an even more diverse array of ion channels based on variations of the structure of voltage-gated K^+ channels (Fig. 4-7B) (Catterall et al., 2002). Ca^{2+}-activated K^+ channels (K_{Ca}) have a core, six-transmembrane-segment architecture similar to K_V channels, and they also contain a region in their C-terminal domain that can bind Ca^{2+} itself or the ubiquitous regulatory protein calmodulin. Binding of Ca^{2+} or Ca^{2+}/calmodulin to the C-terminal domain can act synergistically with membrane depolarization to activate the channel. These channels couple changes in intracellular Ca^{2+} concentration to repolarization of the membrane potential. Some members of the group of channels respond to intracellular Na^+ instead of Ca^{2+}.

Cyclic nucleotide-modulated ion channels (Table 4-2) are not K^+-selective. Nevertheless, their inward current of Na^+ and Ca^{2+} ions is conducted through a channel that is similar in overall architecture to Shaker K^+ channels. This protein family includes the CNG channels, which respond only to

cyclic nucleotides, and the HCN channels, which are activated synergistically by hyperpolarization and cyclic nucleotide binding (Catterall et al., 2002; Matulef & Zagotta, 2003). The CNG channels are involved in signaling of visual and olfactory information. In contrast, the HCN channels are required for normal rhythmic electrical discharges by the sinoatrial node in the heart and the pacemaker cells of the thalamus.

There is also a large family of transient receptor potential (TRP) channels (Catterall et al., 2002; Clapham, 2003) (Table 4-2). These channels, first discovered as the target of a mutation in the *Drosophila* eye, also resemble K_V channels in architecture. However, they are nonselective in most cases, allowing both Na^+ and Ca^{2+} to enter cells when they are active, and they are not strongly affected by membrane potential, even though they have an S4 segment with some positive charges. The activity of this diverse group of channels is regulated in numerous ways, including by lipid messengers, protons, and temperature. These channels transduce taste responses and aversive responses to hot chili peppers, menthol, mustards, and other chemicals. They may also serve as mechanosensory channels under some circumstances. It is likely that we have much more to learn about the physiological roles of this interesting family of ion channels

There are many other kinds of ion channels with different structural backbones and topologies

The channels used in the action potential contrast with those generating slower potential changes at synapses and sensory receptors by having strongly voltage-dependent gating. The other channels have gates controlled by chemical transmitters, intracellular messengers or other energies such as mechanical deformations in touch and hearing. The ionic selectivity of these channels includes a very broad, monovalent anion permeability at inhibitory synapses, a cation permeability (about equal for Na^+ and K^+) at excitatory synapses at the neuromuscular junction and at many sensory transducers, and other, more selective K^+ and Na^+ permeabilities in other synapses. The acetylcholine receptors of the neuromuscular junction and brain, the excitatory glutamate receptors and the inhibitory GABA and glycine receptors all have been solubilized and chemically purified, and the amino acid sequences of their subunits have been determined by the methods of molecular genetics (see Chs. 13–18). The structural features that are responsible for the function of these ligand-gated channels have been recently elucidated by X-ray crystallography.

Recent research shows there is a great diversity of ion channels playing a great diversity of roles in cells throughout the body. We know now that hundreds of genes code for structural components of channels. Beyond its functions in the nervous system, channel activity in endocrine cells regulates the episodes of secretion of insulin from the pancreas and epinephrine from the adrenal gland. Channels initiate and regulate muscle contraction and cell motility. Channels form part of the regulated pathway for the ion movements underlying absorption and secretion of electrolytes by epithelia. Channels also participate in cellular signaling pathways in many other electrically inexcitable cells. Thus, while they are especially prominent in the function of the nervous system, ion channels are actually a basic and ancient component of all cellular life, even bacteria (Hille, 2001).

Ion channels are the targets for mutations that cause genetic diseases

Given the prominent role that ion channels play in control of cellular function, it is not surprising that mutations on ion channels can cause diseases. However, the number of genetic ion channelopathies is remarkable, including genetic forms of epilepsy, migraine headache, ataxia, and chronic pain in the nervous system (Box 4-1). Studies of these rare genetic forms of disease are providing important new insights into the more prevalent (but more difficult to study) spontaneously arising forms of these neurological diseases.

Acknowledgments

The preparation of this chapter was supported by grants NS-08174, NS-15751, and NS-22625 from the National Institutes of Health.

ION CHANNELOPATHIES

Bertil Hille, William A. Catterall

Human geneticists have revealed a surprisingly large number and diversity of genetic diseases caused by mutations in ion channels. This work began with discovery that paramyotonia congenita and hyperkalemic periodic paralysis are caused by mutations in skeletal muscle sodium channels (Venance et al., 2006), and has expanded to include many different types of diseases (Table below; Ashcroft, 2006). Most often these diseases are dominant, so that only one of the two alleles of the ion channel gene is mutated in patients. These mutations may cause gain or loss of channel function. Moreover, different mutations in the same gene can cause different clinical syndromes because of the different mutational effects. A few examples from sodium channelopathies of the nervous system will serve to illustrate these points.

Three different types of periodic paralysis are caused by different mutations in $Na_V1.4$ channels, the primary sodium channel in skeletal muscle (Venance et al., 2006). Paramyotonia congenita is caused by mutations that have a primary effect of slowing the fast inactivation of sodium channels. The mutations therefore cause these channels to stay open too long and to reopen during repolarization of the action potential, resulting in repetitive firing of action potentials and inappropriately long contractions and re-contractions of skeletal muscle. In contrast, hyperkalemic periodic paralysis is caused by mutations that

ION CHANNELOPATHIES (*cont'd*)

impair the slow inactivation process of $Na_V1.4$ channels and therefore cause muscle depolarization, action potential block, and paralysis.

Chronic pain is caused by gain-of-function mutations in $Na_V1.7$ channels, which are important for action potential generation and conduction in pain-sensing neurons in dorsal root ganglia (Dib-Hajj et al., 2010). Impairment of the fast-inactivation process of these sodium channels leads to paroxysmal extreme pain disorder, characterized by intense pain in the rectum, eyes, and mouth. In contrast, mutations that alter the voltage dependence of both activation and slow inactivation of these channels cause inherited erythromelalgia, characterized by burning pain in the extremities. Remarkably, rare families in which both alleles of the $Na_V1.7$ gene have loss-of-function mutations have congenital indifference to pain, in which all sensation of pain is lost. This recessive genetic disease is a serious problem for affected children, who injure themselves without realizing that it is harmful.

Epilepsy is caused by uncontrolled electrical signaling in the brain. Mutations of $Na_V1.1$ channels, one of the three sodium channel types expressed in adult brain, cause multiple clinical forms of epilepsy in children (Catterall et al., 2010). Surprisingly, the most severe form of this group of diseases, severe myoclonic epilepsy of infancy, is caused by loss-of-function mutations that act in a dominant manner. Because sodium channels initiate the action potential, it might be expected that loss-of-function mutations in epilepsy could only reduce electrical excitability. However, studies of this disease in mutant mice have shown that mutation of $Na_V1.1$ channels primarily impairs firing of GABAergic inhibitory neurons (see Chapter 18), which disinhibits action potential firing by excitatory neurons and causes epilepsy (Catterall et al., 2010). In this case, gain-of-function effects on excitability arise at the cellular level because of this failure of inhibitory neuron function.

As the examples from sodium channelopathies of the nervous system shown in the Table below reveal, there is a diversity of mechanisms at both molecular and cellular levels through which mutations in ion channels can cause disease.

Disease Type	Ion Channel Family	Disease Name	Ion Channel Protein	Gene
Epilepsy	Na_V Channel	Severe myoclonic epilepsy of infancy	$Na_V1.1$	SCN1A
		Generalized epilepsy with febrile seizures plus	$Na_V1.1$	SCN1A
		Benign familial neonatal-infantile seizures	$Na_V1.2$	SCN2A
	K_V Channel	Benign familial neonatal seizures	$K_V7.2$	KCNQ2
			$K_V7.3$	KCNQ3
	K_{Ca} Channel	Generalized epilepsy with paroxysmal dyskinesia	$K_{Ca}1.1$	KCNMA1
Pain	Na_V Channel	Familial erythromelagia	$Na_V1.7$	SCN9A
		Paroxysmal extreme pain disorder	$Na_V1.7$	SCN9A
		Congenital indifference to pain	$Na_V1.7$	SCN9A
Migraine Headache	Na_V Channel	Familial hemiplegic migraine type 2	$Na_V1.1$	SCN1A
	Ca_V Channel	Familial hemiplegic migraine type 1	$Ca_V2.1$	CACNA1A
Ataxia	K_V Channel	Episodic ataxia type 1	$K_V1.1$	KCNA1
	Ca_V Channel	Episodic ataxia type 2	$Ca_V2.1$	CACNA1A
		Spinocerebellar ataxia type 6	$Ca_V2.1$	CACNA1A
Mucolipidosis	TRP Channel	Mucolipidosis IV	TRPML1	MCOLN1
Blindness	Ca_V Channel	Congenital stationary night blindness	$Ca_V1.4$	CACNA1F
	CNG Channel	Retinitis pigmentosa	CNGA1	CNGA1
	CNG Channel	Achromatopsia types 2 and 3	CNGA3, CNGB3	CNGA3, CNGB3
Deafness	K_V Channel	Nonsyndromic dominant deafness	$K_V7.4$	KCNQ4
Periodic Paralysis	Na_V Channel	Paramyotonia congenita	$Na_V1.4$	SCN4A
		Hyperkalemic periodic paralysis	$Na_V1.4$	SCN4A

ION CHANNELOPATHIES (*cont'd*)

Disease Type	Ion Channel Family	Disease Name	Ion Channel Protein	Gene
		Hypokalemic periodic paralysis type 2	$Na_V1.4$	SCN4A
	Ca_V Channel	Hypokalemic periodic paralysis type 1	$Ca_V1.1$	CACNA1S
Cardiac Arrhythmia	Na_V Channel	Brugada syndrome	$Na_V1.5$	SCN5A
	K_V Channel	Long QT syndrome type 3	$Na_V1.5$	SCN5A
		Long QT syndrome type 1 (plus deafness)	$K_V7.1$	KCNQ1
		Long QT syndrome type 2		KCNH2
	Ca_V Channel	Timothy syndrome (long QT interval plus developmental defects and autism)	$Ca_V1.2$	CACNA1C
	Kir Channel	Andersen-Tawil syndrome (cardiac arrhythmia with developmental defects and periodic paralysis)	Kir2.1	KCNJ2
Kidney Failure	Kir Channel	Bartter's syndrome (salt-wasting)	Kir 1.1	KCNJ1
	TRP Channel	Autosomal dominant polycystic kidney disease	TRPP2	TRPP2
		Focal segmental glomerulosclerosis	TRPC6	TRPC6
Hyperinsulinemia and Diabetes	Kir Channel	Congenital hyperinsulinemia	Kir6.2	KCNJ11
		Neonatal diabetes	Kir6.2	KCNJ11

References

Agnew, W. S. (1984). Voltage-regulated sodium channel molecules. *Annual Review of Biochemistry*, *46*, 517–530.

Armstrong, C. M. (1981). Sodium channels and gating currents. *Physiological Reviews*, *61*, 644–683.

Armstrong, C. M. (2003). Voltage gated K channels. *Science's STKE*, *2003*(188), p. re10.

Ashcroft, F. M. (2006). From molecule to malady. *Nature*, *440*, 440–447.

Barchi, R. L. (1984). Voltage-sensitive sodium ion channels. Molecular properties and functional reconstitution. *Trends in Biochemical Sciences*, *9*, 358–361.

Bezanilla, F. (2000). The voltage sensor in voltage dependent ion channels. *Physiological Reviews*, *80*, 555–592.

Catterall, W. A. (1980). Neurotoxins acting on sodium channels. *Annual Review of Pharmacology and Toxicology*, *20*, 15–43.

Catterall, W. A. (1986). Molecular properties of voltage-sensitive sodium channels. *Annual Review of Biochemistry*, *55*, 953–985.

Catterall, W. A. (2000). From ionic currents to molecular mechanisms: the structure and function of voltage-gated sodium channels. *Neuron*, *26*, 13–25.

Catterall, W. A. (2000). Structure and regulation of voltage-gated calcium channels. *Annual Review of Cell and Developmental Biology*, *16*, 521–555.

Catterall, W. A., Gutman, G. A., & Chandy, K. G. (2002). *The IUPHAR compendium of voltage-gated ion channels*. Leeds, UK: IUPHAR Media, 2002. Retrieved from <www.iuphar-db.org/iuphar-ic>.

Catterall, W. A., Kalume, F., & Oakley, J. C. (2010). $Na_v1.1$ channels and epilepsy. *Journal of Physiology*, *588*, 1849–1859.

Clapham, D. E. (2003). TRP channels as cellular sensors. *Nature*, *426*, 517–524.

Dib-Hajj, S. D., Cummins, T. R., Black, J. A., & Waxman, S. G. (2010). Sodium channels in normal and pathological pain. *Annual Review of Neuroscience*, *33*, 325–347.

Doupnik, C. A., Davidson, N., & Lester, H. A. (1995). The inward rectifier potassium channel family. *Current Opinion in Neurobiology*, *5*, 268–277.

Doyle, D. A., Morais Cabral, J., Pfuetzner, R. A., Kuo, A., Gulbis, J. M., Cohen, S. L., et al. (1998). The structure of the potassium channel: Molecular basis of K^+ conduction and selectivity. *Science*, *280*, 69–77.

Gandhi, C. S., & Isacoff, E. Y. (2002). Molecular models of voltage sensing. *Journal of General Physiology*, *120*, 455–463.

Goldin, A. L., Snutch, T., Lübbert, H., Dowsett, A., Marshall, J., Auld, V., et al. (1986). Messenger RNA coding for only the α-subunit of the rat brain Na channel is sufficient for expression of functional channels of *Xenopus* oocytes. *Proceedings of the National Academy of Sciences of the United States of America*, *83*, 7503–7507.

Goldstein, S. A., Bockenhauer, D., O'Kelly, I., Zilberbeg, N., et al. (2001). Potassium leak channels and the KCNK family of two-P-domain subunits. *Nature Reviews Neuroscience*, *2*, 175–184.

Guy, H. R., & Conti, F. (1990). Pursuing the structure and function of voltage-gated channels. *Trends in Neurosciences*, *13*, 201–206.

Hamill, O. P., Marty, A., Neher, E., Sakmann, B., Sigworth, F. J., et al. (1981). Improved patch-clamp techniques for high-resolution current recording from cells and cell-free membrane patches. *Pflügers Archiv*, *391*, 85–100.

Heinemann, S. H., Terlau, H., Stühmer, W., Imoto, K., Numa, S., et al. (1992). Calcium channel characteristics conferred on the sodium channel by single mutations. *Nature*, *356*, 441–443.

Hille, B. (1997). Ionic basis of resting and action potentials. In J. M. (1997). Brookhart (Ed.), *Handbook of physiology* (Vol. 1, pp. 99–136). Washington, DC: American Physiological Society.

Hille, B. (2001). *Ion channels of excitable membranes* (3rd ed.). Sunderland, MA: Sinauer Associates.

Hodgkin, A. L. (1964). *The conduction of the nervous impulse*. Springfield, IL: Charles C. Thomas.

Hodgkin, A. L., & Huxley, A. F. (1952). A quantitative description of membrane current and its application to conduction and excitation in nerve. *Journal of Physiology (London)*, *117*, 500–544.

Hofmann, F., Biel, M., & Flockerzi, V. (1994). Molecular basis for Ca^{2+} channel diversity. *Annual Review of Neuroscience*, *17*, 399–418.

Hoshi, T., Zagotta, W., & Aldrich, R. W. (1990). Biophysical and molecular mechanisms of Shaker potassium channel inactivation. *Science*, *250*, 533–538.

Isom, L. L., De Jongh, K. S., & Catterall, W. A. (1994). Auxiliary subunits of voltage-gated ion channels. *Neuron*, *12*, 1183–1194.

Jan, L. Y., & Jan, Y. N. (1997). Voltage-gated and inwardly rectifying potassium channels. *Journal of Physiology*, *505*, 267–282.

Jiang, Y., Lee, A., Chen, J., Cadene M., Chait B. T., Mackinnon, R., et al. (2002). Crystal structure and mechanism of a calcium-gated potassium channel. *Nature*, *417*, 515–522.

Long, S. B., Campbell, E. B., & MacKinnon, R. (2005). Crystal structure of a mammalian voltage-dependent Shaker family K^+ channel. *Science*, *309*, 897–903.

Matulef, K., & Zagotta, W. N. (2003). Cyclic nucleotide-gated ion channels. *Annual Review of Cell Developmental Biology*, *19*, 23–44.

Miller, C. (1990). *Annus mirabilis* for potassium channels. *Science*, *252*, 1092–1096.

Nicholls, J. G., Martin, A. R., Wallace, B. G., & Fuchs, P. A. (2001). *From neuron to brain* (4th ed.). Sunderland, MA: Sinauer Associates.

Noda, M., Ikeda, T., Kayano, T., Suzuki, H., Takeshima, H., Kurasaki, M., et al. (1986). Existence of distinct sodium channel messenger RNAs in rat brain. *Nature*, *320*, 188–192.

Noda, M., Ikeda, T., Suzuki, H., Takeshima, H., Takahashi, T., Kuno, M., et al. (1886). Expression of functional sodium channels from cloned cDNA. *Nature*, *322*, 826–828.

Pongs, O. (1999). Voltage-gated potassium channels: From hyperexcitability to excitement. *FEBS Letters*, *452*, 31–35.

Stühmer, W., Conti, F., Suzuki, H., Wang, X. D., Noda, M., Yahagi, N., et al. (1989). Structural parts involved in activation and inactivation of the sodium channel. *Nature*, *339*, 597–603.

Terlau, H., Heinemann, S. H., Stühmer, W., Pusch, M., Conti, F., Imoto, K., et al. (1991). Mapping the site of block by tetrodotoxin and saxitoxin of sodium channel II. *FEBS Letters*, *293*, 93–96.

Vassilev, P., Scheuer, T., & Catterall, W. A. (1998). Identification of an intracellular peptide segment involved in sodium channel inactivation. *Science*, *241*, 1658–1661.

Venance, S. L., Cannon, S. C., Fialho, D., Fontaine, B., Hanna, M. G., Ptacek, L. J., et al. (2006). The primary periodic paralyses: Diagnosis, pathogenesis and treatment. *Brain*, *129*, 8–17.

West, J. W., Patton, D. E., Scheuer, T., Wang, Y., Goldin, A. L., Catterall, W. A., et al. (1992). A cluster of hydrophobic amino acid residues required for fast sodium channel inactivation. *Proceedings of the National Academy of Sciences of the United States of America*, *89*, 10910–10914.

Yang, N. B., George, A. L., Jr., & Horn, R. (1996). Molecular basis of charge movement in voltage-gated sodium channels. *Neuron*, *16*, 113–122.

Yarov-Yarovoy, V., Baker, D., & Catterall, W. A. (2006). Voltage sensor conformations in the open and closed states in ROSETTA structural models of K^+ channels. *Proceedings of the National Academy of Sciences of the United States of America*, *103*, 7292–7297.

Zagotta, W., Hoshi, T., & Aldrich, R. W. (1990). Restoration of inactivation in mutants of Shaker potassium channels by a peptide derived from Sh B. *Science*, *250*, 568–571.

Zhao, Y., Yarov-Yarovoy, V., Scheuer, T., Catterall, W. A., et al. (2004). A gating hinge in Na^+ channels: A molecular switch for electrical signaling. *Neuron*, *41*, 859–865.